

Polaron transport and lattice dynamics in colossal magnetoresistance manganites

J. D. Lee and B. I. Min

*Department of Physics, Pohang University of Science and Technology,
Pohang 790-784, Korea*

Based on the model combining the spin double exchange and the lattice polaron, we have studied the colossal magnetoresistance phenomena observed in perovskite manganites $R_{1-x}A_xMnO_3$. First, effects of both the double exchange and the electron-phonon interaction on the transport property are investigated. We have evaluated the temperature dependent resistance and the magnetoresistance using the Kubo formula, and examined the crossover from tunneling to hopping regime of small polarons. Second, effects of the double exchange interaction on the lattice degree of freedom are explored. It is found that both the hardening of the phonon frequency and the reduction of the phonon damping take place with decreasing the temperature.

PACS: 71.38.+i, 72.15.Gd, 75.30.Kz

I. INTRODUCTION

The "colossal" magnetoresistance (CMR) manganites $R_{1-x}A_xMnO_3$ ($R = \text{La, Pr, Nd}$; $A = \text{Ca, Ba, Sr, Pb}$) have recently attracted considerable attention due to scientific interest and potential applicability of their very large magnetoresistance (MR) for $0.2 \lesssim x \lesssim 0.5$ [1–3]. The most essential feature of their magnetic and transport behaviors is the existence of metallic conductivity and ferromagnetism. The magnetic transition at T_c is closely connected with the resistivity peak at T_P corresponding to an insulator-metal transition ($T_c \sim T_P$). The correlation between ferromagnetism and metallic conductivity in $R_{1-x}A_xMnO_3$ was explained by Zener [4] in terms of the double exchange mechanism. There are mixed valent Mn ions (Mn^{3+} and Mn^{4+}) as a consequence of hole doping by substituting R^{3+} with A^{2+} . In the double exchange model, conduction electrons in the partially filled e_g levels of the d band are strongly coupled with the tightly bound d electrons in the t_{2g} levels by the on-site Hund's coupling, and mediate the ferromagnetic exchange interaction between the nearest neighbor $S = \frac{3}{2}$ local spins formed from three d electrons in the core-like t_{2g} levels [4,5].

Transport properties have been studied within the double exchange mechanism in favor of a magnetic polaron [6–8]. Recently, Millis *et al.* [9] reported that the effective carrier-spin interaction involved in the ordinary double exchange Hamiltonian is too weak to produce the magnetic polaron effects. Instead, they suggested lattice polaron effects due to a strong electron-phonon interaction as a necessary additional extension [10]. They investigated a model of electrons, Jahn-Teller coupled to localized classical oscillators, within the dynamical mean field theory. Röder *et al.* [11] also examined the combined influence of the electron-phonon interaction and the double exchange on T_c using the variational wave function techniques. But they could not treat the polaron transport and the lattice dynamics on an equal footing. In fact, the contribution of the lattice polaron to carrier mobility was pointed out earlier by Goodenough [12].

There are many experimental evidences suggesting importance of the electron-lattice coupling in manganese oxides [13–17]. Near T_c , dramatic changes are observed in the lattice degree of freedom - the anomalous lattice expansion beyond Grüneisen law [14], and the shift of phonon frequency [15–17], which all reflect that the lattice is closely related to the electronic and magnetic properties. However, detailed understanding of the interplay between the lattice dynamics and the electronic and magnetic properties remains to be resolved.

In this paper, we have addressed two questions; i) what is the role of the electron-phonon interaction in CMR systems which are known to have the double exchange interaction, and reversely, ii) how the double exchange interaction affects the lattice dynamics through the electron-phonon interaction. For these purposes, we first investigate effects of both the double exchange and the electron-phonon interaction on transport and magnetic properties. Employing the Kubo formula, we have determined the temperature dependent resistance and the magnetoresistance, and examined the crossover from a metallic tunneling state to an insulating hopping state in the small polaron transport. Second, to characterize the lattice dynamics in CMR compounds, we have considered the phonon degree of freedom in the presence of the double exchange interaction. We have studied the renormalization of the phonon frequency and the phonon damping constant.

This paper is organized as follows. In section II, we present the model of conduction electrons coupled to phonons as well as the localized ionic spins in terms of the double exchange, whereby the temperature dependent resistance and the magnetoresistance are evaluated from the Kubo formula. In section III, we examine the double exchange

effects on the lattice degree of freedom. Finally, conclusions follow in section IV. Detailed calculational steps are given in Appendix.

II. POLARON TRANSPORT

Since Zener [4] has proposed an interaction between spins of magnetic ions named "double exchange", Anderson and Hasegawa [5] studied this mechanism in a system of Mn ions and a mobile electron with the transfer t between two Mn ions and the strong intra-atomic exchange integral J . When J is much larger than t , motion of the mobile electrons in $R_{1-x}A_xMnO_3$ is described by the following double exchange Hamiltonian,

$$\mathcal{H}_{DE} = \sum_{ij} t_{ij} \cos \frac{\theta_{ij}}{2} c_i^\dagger c_j, \quad (1)$$

where the hopping t_{ij} connects neighboring sites, and θ_{ij} is the angle between the directions of ionic spins at sites i and j . An exact quantum mechanical calculation gives $\cos \frac{\theta_{ij}}{2} = \frac{S_0+1/2}{2S+1}$, where S is the spin of a Mn ion and S_0 is the total spin of S_i , S_j and the conduction electron spin. In this study, we treat the double exchange part within the mean field theory following Kubo and Ohata [6], in which $\cos \frac{\theta_{ij}}{2}$ is replaced by its thermodynamic average $\langle \cos \frac{\theta_{ij}}{2} \rangle$ determined by minimizing the free energy of the spin system. Then the propagation of an electron can be described as if it were moving in a mean field of highly disordered configurations of ionic spins. This approximation is known to work well at finite temperature, except for the very low temperature region ($T \sim 0K$) where the spin dynamics becomes important. Within the present mean field theory, the double exchange plays a role, through $\langle \frac{S_0+1/2}{2S+1} \rangle \equiv \gamma(T)$, of increasing the bandwidth as T decreases below T_c , accompanied by the ferromagnetic ordering (see Fig. 1(a)).

In addition to the double exchange, the conduction electrons are scattered by the Mn-O ionic motions in the MnO_6 octahedra, which gives rise to a very strong electron-phonon interaction. The effective Hamiltonian incorporating the electron-phonon interaction is written as,

$$\mathcal{H} = t \langle \cos \frac{\theta}{2} \rangle \sum_{i\delta} c_{i+\delta}^\dagger c_i + \sum_{\vec{q}} \omega_{\vec{q}} a_{\vec{q}}^\dagger a_{\vec{q}} + \sum_{i\vec{q}} c_i^\dagger c_i e^{i\vec{q} \cdot \vec{R}_i} M_{\vec{q}} (a_{\vec{q}} + a_{-\vec{q}}^\dagger). \quad (2)$$

Here we adopt a model in which the single e_g orbital is coupled to phonons assuming the electronically active e_g band to be split, as in Röder *et al.*'s [11]. The present assumption is expected to be more effective if the model were generalized to include another physics such as the on-site Coulomb interaction, which might remove possible mid-gap states away from the Fermi level [10].

The dc conductivity σ can be obtained from the optical conductivity $\sigma(\omega)$ by taking the $\omega \rightarrow 0$ limit, and $\sigma(\omega)$ can be determined by using the Kubo formula of the current-current correlation function,

$$\sigma(\omega) = \frac{1 - e^{-\beta\omega}}{2\omega} \int_{-\infty}^{\infty} d\tau e^{i\omega\tau} \langle J_\alpha^\dagger(\tau) J_\alpha(0) \rangle. \quad (3)$$

Since the current operator \vec{J} in narrow band systems is given by

$$\vec{J} = it \langle \cos \frac{\theta}{2} \rangle e \sum_{j\delta} \hat{\delta} c_{j+\delta}^\dagger c_j, \quad (4)$$

σ explicitly involves the four-site correlation function,

$$\sigma = \frac{\beta}{2} t^2 \langle \cos \frac{\theta}{2} \rangle^2 e^2 \sum_{\delta\delta'} \sum_{jj'} (\hat{\delta} \cdot \hat{\delta}') \int_{-\infty}^{\infty} d\tau \langle c_j^\dagger(\tau) c_{j+\delta}(\tau) c_{j'+\delta'}^\dagger c_{j'} \rangle. \quad (5)$$

In the isotropic case, the resistivity ρ corresponds to the inverse of σ , $\rho = 1/\sigma$.

To evaluate σ , let's consider the well-known polaron canonical transformation [18]; $\bar{\mathcal{H}} = e^S \mathcal{H} e^{-S}$ with $S = -\sum_{j\vec{q}} c_j^\dagger c_j e^{i\vec{q} \cdot \vec{R}_j} \frac{M_{\vec{q}}}{\omega_{\vec{q}}} (a_{\vec{q}} - a_{-\vec{q}}^\dagger)$. The transformed Hamiltonian $\bar{\mathcal{H}}$ is given by

$$\bar{\mathcal{H}} = t \langle \cos \frac{\theta}{2} \rangle \sum_{j\delta} c_{j+\delta}^\dagger c_j X_{j+\delta}^\dagger X_j + \sum_{\vec{q}} \omega_{\vec{q}} a_{\vec{q}}^\dagger a_{\vec{q}} - \Delta \sum_j c_j^\dagger c_j, \quad (6)$$

with $X_j = \exp \left[\sum_{\vec{q}} e^{i\vec{q}\cdot\vec{R}_j} \frac{M_q}{\omega_q} (a_{\vec{q}} - a_{-\vec{q}}^\dagger) \right]$ and $\Delta = \sum_{\vec{q}} \frac{M_q^2}{\omega_q}$. Inserting $e^S e^{-S} = 1$ between each electron operator in Eq.(5), and using $e^S c_j e^{-S} = c_j X_j$ and $e^S c_j^\dagger e^{-S} = c_j^\dagger X_j^\dagger$, one gets

$$\sigma = \frac{\beta}{2} t^2 \langle \cos \frac{\theta}{2} \rangle^2 e^2 \sum_{\delta\delta'} \sum_{jj'} (\hat{\delta} \cdot \hat{\delta}') \int_{-\infty}^{\infty} d\tau \langle c_j^\dagger(\tau) c_{j+\delta}(\tau) c_{j'+\delta'}^\dagger c_{j'} X_j^\dagger(\tau) X_{j+\delta}(\tau) X_{j'+\delta'}^\dagger X_{j'} \rangle. \quad (7)$$

The intricate correlation function of Eq.(7) should be evaluated under the transformed Hamiltonian $\bar{\mathcal{H}}$. Calculation can be further simplified with an approximation replacing the first term of Eq.(6) by $t \langle \cos \frac{\theta}{2} \rangle \sum_{j\delta} \langle X_{j+\delta}^\dagger X_j \rangle c_{j+\delta}^\dagger c_j$. This approximation is quite reasonable in view of that the coherent band-like motion of the polarons arises from the quantum mechanical tunneling between sites without changing the phonon numbers, which is governed by the matrix elements of $\langle n_{\mathbf{q}} | X_{j+\delta}^\dagger X_j | n_{\mathbf{q}} \rangle$ [19]. With increasing T , the polaron bandwidth decreases exponentially due to the term $\langle X_{j+\delta}^\dagger X_j \rangle (\equiv \Gamma(T))$,

$$\Gamma(T) = \exp \left[- \sum_{\vec{q}} |u_{\vec{q}}|^2 (N_q + 1/2) \right], \quad (8)$$

where $u_{\vec{q}} \equiv (M_q/\omega_q)(e^{i\vec{q}\cdot\vec{\delta}} - 1)$ (see Fig. 1(b)). Under the above approximation, the mean field scheme of Kubo and Ohata [6] can be generalized to include the phonon contributions which drastically reduce the magnetic transition temperature T_c [11], whereas the temperature dependent behavior of $\langle \cos \frac{\theta}{2} \rangle (\equiv \gamma(T))$ does not appreciably change.

With the approximate Hamiltonian $\bar{\mathcal{H}}$ incorporating both $\gamma(T)$ and $\Gamma(T)$, the complicated four-site correlation function in Eq.(7) can be disentangled into $\langle c_j^\dagger(\tau) c_{j+\delta}(\tau) c_{j'+\delta'}^\dagger c_{j'} \rangle \langle X_j^\dagger(\tau) X_{j+\delta}(\tau) X_{j'+\delta'}^\dagger X_{j'} \rangle$. These correlation functions and σ can be evaluated in the straightforward fashion. Detailed calculational procedures are provided in Appendix. From Eq.(A12), the dc conductivity σ is given as follows,

$$\begin{aligned} \sigma &= \frac{\beta}{2} t^2 \gamma(T)^2 e^2 \sum_{\delta\delta'} \sum_{jj'} (\hat{\delta} \cdot \hat{\delta}') \sum_{\vec{k}_1 \vec{k}_2} n_{\vec{k}_1} (1 - n_{\vec{k}_2}) e^{-i\vec{k}_1 \cdot (\vec{R}_j - \vec{R}_{j'})} e^{i\vec{k}_2 \cdot (\vec{R}_j - \vec{R}_{j'} + \vec{\delta} - \vec{\delta}')} \\ &\times e^{(\tilde{t}_{\vec{k}_1} - \tilde{t}_{\vec{k}_2})/2T} e^{-(\tilde{t}_{\vec{k}_1} - \tilde{t}_{\vec{k}_2})^2/4\zeta(j,j',\vec{\delta},\vec{\delta}';T)} e^{-\xi(T)} e^{\eta(j,j',\vec{\delta},\vec{\delta}';T)} [\pi/\zeta(j,j',\vec{\delta},\vec{\delta}';T)]^{1/2}, \end{aligned} \quad (9)$$

with a renormalized polaron band, $\tilde{t}_{\vec{k}} = t\gamma(T)\Gamma(T) \sum_{\delta} e^{-i\vec{k}\cdot\vec{\delta}} - \Delta$. Explicit expressions of $\zeta(j,j',\vec{\delta},\vec{\delta}';T)$, $\xi(T)$, and $\eta(j,j',\vec{\delta},\vec{\delta}';T)$ are given in Appendix. Keeping in mind that the auto-correlation function is most dominant for $j = j'$ and $\vec{\delta} = \vec{\delta}'$, σ is more simply obtained in the following form

$$\sigma = \frac{\beta}{2} t^2 \gamma(T)^2 e^2 N z \sum_{\vec{k}_1 \vec{k}_2} n_{\vec{k}_1} (1 - n_{\vec{k}_2}) e^{(\tilde{t}_{\vec{k}_1} - \tilde{t}_{\vec{k}_2})/2T} e^{-(\tilde{t}_{\vec{k}_1} - \tilde{t}_{\vec{k}_2})^2/4\zeta(T)} e^{-\xi(T)} e^{\eta(T)} (\pi/\zeta(T))^{1/2}. \quad (10)$$

Here z is the number of the nearest neighbors, $n_{\vec{k}}$ and N_q are the fermion and boson distribution function, respectively, and $\xi(T)$, $\zeta(T)$, and $\eta(T)$ are also given by

$$\xi(T) = \sum_{\vec{q}} |u_{\vec{q}}|^2 (1 + 2N_q), \quad (11)$$

$$\zeta(T) = \sum_{\vec{q}} \omega_q^2 |u_{\vec{q}}|^2 [N_q(N_q + 1)]^{1/2}, \quad (12)$$

$$\eta(T) = 2 \sum_{\vec{q}} |u_{\vec{q}}|^2 [N_q(N_q + 1)]^{1/2}. \quad (13)$$

Now let's investigate the qualitative behavior of ρ . One can carry out the numerical calculation of Eq.(10), assuming the simple square density of states (DOS) $\mathcal{D}(\epsilon)$,

$$\mathcal{D}(\epsilon) = \frac{N(1-x)}{\epsilon_F}, \quad -\frac{W}{2} \leq \epsilon \leq \frac{W}{2}. \quad (14)$$

Here the bandwidth W is given by $w\gamma(T)\Gamma(T)$ (w is the bare electron bandwidth and estimated to be $w = 12|t| \sim 2\text{eV}$ from the band structure calculation), and the Fermi energy ϵ_F is $w\gamma(T)\Gamma(T)(1-x)$ with x being the doping concentration. These treatments of DOS are based on the assumption that only the lower one of the split e_g bands is active. We also assume that the most relevant phonon mode is the optical mode ($\sim \omega_0$) which might be involved in the Jahn-Teller coupling.

Numerical results for the resistivity are provided in Fig. 2. Two dashed lines represent resistivities of the polaron only model with given bandwidths of $\tilde{t}_{\text{up}} (= w\Gamma(T))$ and $\tilde{t}_{\text{low}} (= 0.75w\Gamma(T))$. Here \tilde{t}_{up} and \tilde{t}_{low} correspond, respectively, to upper and lower limits of the double exchange factor $\gamma(T)$. In both cases, ρ 's exhibit peaks as a function of T , and the larger band width \tilde{t}_{up} yields a smaller ρ with a peak at higher temperature. The resistivity peak as a function of T corresponds to the crossover from a quantum tunneling of the metallic phase to a self-trapped small polaron hopping of the insulating phase. Such features are characteristics of polaron systems, which are indeed observed in many oxide systems. In the high T limit, the resistivity has a thermal activation form of $\exp(\Delta_g/T)$, characteristic of the semiconducting phase [18]. Now taking the double exchange into account, the polaron bandwidth increases with decreasing T due to $\gamma(T)$, and accordingly the resistivity is given by the solid line (in Fig. 2) with a peak at T_c connecting the two polaron resistivity curves. This figure clearly demonstrates that the semiconducting behavior above T_c is attributed to self-trapped lattice small polarons, and that the rapid fall-off in the resistivity below T_c is attributed to the double exchange mechanism in addition to the lattice polaron effect. Thus, the combined model of the double exchange and the polaron provides a good description of the resistance anomaly observed in the experiment. The coincidence of the resistivity peak position T_P with T_c originates from the mean field treatment of $\gamma(T)$ which neglects the fluctuation in the hopping of conduction electrons.

Effects of the external magnetic field can also be taken into account in $\gamma(T)$ through the modified free energy due to the magnetic field. The behaviors of the MR's are shown in the inset of Fig. 2. With increasing the field intensity, the resistivity decreases and the peak position shifts to a higher T , and so the negative MR results. These results are quite consistent with the experimental observations. The MR peak T_{MR} is located near the resistivity peak T_P . In fact, T_{MR} , T_P , and T_c are the same in the present mean field treatment. It should be noticed that the magnitudes of the MR's in the figure are not large enough to explain the experimental CMR data quantitatively, suggesting that additional treatments might be required. One possibility is to incorporate the half-metallic nature of the ferromagnetic manganites [20,21], which is expected to suppress largely the spin-disorder scattering under the external magnetic field.

III. LATTICE DYNAMICS

As mentioned before, the phonon frequency becomes hardened as T decreases below T_c [15–17]. Interestingly, the phonon hardenings are observed for both optical and acoustic phonons in these systems. These frequency shifts are considered to be due to the change in the electron screening as T is lowered below T_c . The hardening occurs in the metallic region ($T \lesssim T_c$), *i.e.*, in the band-type tunneling regime where Rayleigh-Schrödinger perturbation theory is valid [18]. Therefore it is expected that the change of the bandwidth due to the double exchange factor $\gamma(T)$ modifies the electron screening below T_c . Note that the previous approximation for the canonically transformed Hamiltonian $\tilde{\mathcal{H}}$ corresponds to neglecting the phonon frequency renormalization, which seems to be too small to cause any appreciable change in the transport properties. In the metallic regime, the screening of the conduction electrons will be more easily described by the original Hamiltonian \mathcal{H} of Eq.(2) rather than the polaron Hamiltonian $\tilde{\mathcal{H}}$ of Eq.(6).

The renormalized phonon frequency $\tilde{\omega}_q$ and the damping constants α_q can be obtained from the following equation [22]

$$(\tilde{\omega}_q - i\alpha_q)^2 = \omega_q^2 - 2\omega_q|M_q|^2\mathcal{F}(\vec{q}, \tilde{\omega}_q + i0^+), \quad \tilde{\omega}_q \gg \alpha_q, \quad (15)$$

where the electron screening function $\mathcal{F}(\vec{q}, \tilde{\omega}_q)$ is given by

$$\mathcal{F}(\vec{q}, \tilde{\omega}_q) = \sum_{\vec{q}} \frac{n_{\vec{k}} - n_{\vec{k}+\vec{q}}}{\gamma(T)(t_{\vec{k}+\vec{q}} - t_{\vec{k}}) - \tilde{\omega}_q}, \quad t_{\vec{k}} = t \sum_{\delta} e^{i\vec{k}\cdot\vec{\delta}}. \quad (16)$$

The real part of both sides of Eq.(15) yields

$$\tilde{\omega}_q^2 \simeq \omega_q^2 - 2\omega_q|M_q|^2 \frac{1}{\gamma(T)} \sum_{\vec{k}} \frac{n_{\vec{k}} - n_{\vec{k}+\vec{q}}}{t_{\vec{k}+\vec{q}} - t_{\vec{k}}}. \quad (17)$$

It is important to note that the term $\sum_{\vec{q}}(n_{\vec{k}} - n_{\vec{k}+\vec{q}})/(t_{\vec{k}+\vec{q}} - t_{\vec{k}})$ has very weak temperature dependences ($\sim C + \mathcal{O}(T/E_F)^2$, E_F being the Fermi level determined from $t_{\vec{k}}$). Hence the T -dependence of $\tilde{\omega}_q$ comes dominantly from $\gamma(T)$, and Eq.(17) can be written as $\tilde{\omega}_q = \omega_q(1 - \bar{\beta}/\gamma(T))^{1/2}$, where $\bar{\beta}$ contains all the T -independent terms. An explicit calculation of $\bar{\beta}$ is not available, but the order of its magnitude should be very small, $\mathcal{O}(|M_q|^2/(\omega_q E_F)) \sim \mathcal{O}(10^{-2})$. In Fig. 3(a), T -dependent behaviors of $\tilde{\omega}_q$ are plotted with respect to the external magnetic field strength H , and compared with the available experiment [16] in the inset. It is seen that the frequency hardenings with decreasing T and with increasing H are qualitatively well explained. However, it is also apparent that some deviations exist between calculational and experimental results, particularly, near T_c . These discrepancies might be ascribed to the mean field treatment of $\gamma(T)$. Including spin correlation effects in calculating $\gamma(T)$ is expected to improve the agreement. It should also be noted that the phonon frequency hardening of Eq.(17) would be valid for both acoustic and optical phonon modes consistently with the experiments, because we have assumed the general form of the electron-phonon interaction in Eq.(2).

Taking the imaginary part for both sides of Eq.(15), one gets the phonon damping parameter α_q ,

$$2\alpha_q\tilde{\omega}_q = 2\omega_q|M_q|^2 \frac{1}{\gamma(T)} \text{Im} \sum_{\vec{k}} \frac{n_{\vec{k}} - n_{\vec{k}+\vec{q}}}{t_{\vec{k}+\vec{q}} - t_{\vec{k}} - \tilde{\omega}_q/\gamma(T) - i0^+}. \quad (18)$$

The imaginary part of the screening function is easily calculated by considering a parabolic electron band $t_{\vec{k}} = t \sum_{\delta} e^{i\vec{k}\cdot\delta} \simeq |t|\delta^2 k^2$,

$$2\alpha_q = 2\omega_q|M_q|^2 \frac{\pi}{2} \frac{\mathcal{D}(E_F)}{v_F q} \frac{1}{\gamma(T)^2}, \quad (19)$$

where $\mathcal{D}(E_F)$ and v_F are determined from the parabolic band, $|t|\delta^2 k^2$. In Fig. 3(b), T -dependent behaviors of α_q are presented. Our results predict that the phonon damping parameter decreases with decreasing T , implying that the phonon is more sharply defined below T_c . This feature in CMR systems is quite different from conventional observations of increased phonon damping parameter below T_c for magnetic or strongly correlated systems. To our knowledge, no experimental reports are available yet on the phonon damping parameter. We think that the sound attenuation experiment will provide a better understanding of the nature of the electron-phonon interaction in CMR systems.

IV. CONCLUSIONS

We have extended the double exchange model to incorporate the strong electron-phonon interaction, and investigated transport and magnetic properties of CMR manganese oxides $R_{1-x}A_x\text{MnO}_3$. We have found that the semiconducting behavior in manganites above T_c is attributed to the effect of self-trapped lattice small polarons, and that the rapid fall-off in the resistivity below T_c is attributed to the combined effect of coherent lattice polarons and the increased bandwidth via the double exchange mechanism accompanied by the ferromagnetic ordering of magnetic ions. Further, we have explored effects of the double exchange on the phonon degrees of freedom. The temperature dependent hardening of the phonon mode frequency observed in experiments is well described, and the reduction of the phonon damping constant is predicted below T_c .

ACKNOWLEDGMENTS

This work was supported by the Korea Research Foundation, and in part by the BSRI program of the Korean Ministry of Education and the POSTECH special fund. Helpful discussions with Y.H. Jeong and T.W. Noh are greatly appreciated.

APPENDIX: CALCULATION OF dc CONDUCTIVITY σ

To evaluate the dc conductivity σ , one should evaluate correlation functions of electrons and phonons under the Hamiltonian $\bar{\mathcal{H}}$. Defining simply Λ and Λ' as

$$\Lambda = e^{i\vec{q}\cdot\vec{R}_j}(e^{i\vec{q}\cdot\vec{\delta}} - 1)\frac{M_q}{\omega_q}, \quad \Lambda' = e^{i\vec{q}\cdot\vec{R}'_j}(e^{i\vec{q}\cdot\vec{\delta}'} - 1)\frac{M_q}{\omega_q}, \quad (\text{A1})$$

$X_j^\dagger(\tau)X_{j+\delta}(\tau)X_{j'+\delta'}X_{j'}$ is given by

$$X_j^\dagger(\tau)X_{j+\delta}(\tau)X_{j'+\delta'}X_{j'} = \prod_{\vec{q}} e^{-\frac{1}{2}(|\Lambda|^2+|\Lambda'|^2)} e^{\Lambda^* a_{\vec{q}}^\dagger e^{i\omega_q \tau}} e^{-\Lambda a_{\vec{q}} e^{-i\omega_q \tau}} e^{-\Lambda'^* a_{\vec{q}}^\dagger} e^{\Lambda' a_{\vec{q}}}. \quad (\text{A2})$$

Using $e^{-\Lambda a_{\vec{q}} e^{-i\omega_q \tau}} e^{-\Lambda'^* a_{\vec{q}}^\dagger} = e^{-\Lambda'^* a_{\vec{q}}^\dagger} e^{-\Lambda a_{\vec{q}} e^{-i\omega_q \tau}} e^{\Lambda \Lambda'^* e^{-i\omega_q \tau}}$, we see

$$X_j^\dagger(\tau)X_{j+\delta}(\tau)X_{j'+\delta'}X_{j'} = \prod_{\vec{q}} e^{-\frac{1}{2}(|\Lambda|^2+|\Lambda'|^2)} e^{\Lambda \Lambda'^* e^{-i\omega_q \tau}} e^{\Lambda^* a_{\vec{q}}^\dagger} e^{-\lambda a_{\vec{q}}}, \quad (\text{A3})$$

where $\lambda \equiv \Lambda e^{-i\omega_q \tau} - \Lambda'$. Under the noninteracting phonon Hamiltonian, the thermodynamic average of $\langle e^{\Lambda^* a_{\vec{q}}^\dagger} e^{-\lambda a_{\vec{q}}} \rangle$ is given by [18]

$$\langle e^{\Lambda^* a_{\vec{q}}^\dagger} e^{-\lambda a_{\vec{q}}} \rangle = e^{-|\lambda|^2 N_q}, \quad N_q = \frac{1}{e^{\beta\omega_q} - 1}. \quad (\text{A4})$$

Then $\langle X_j^\dagger(\tau)X_{j+\delta}(\tau)X_{j'+\delta'}X_{j'} \rangle$ is obtained as follows

$$\langle X_j^\dagger(\tau)X_{j+\delta}(\tau)X_{j'+\delta'}X_{j'} \rangle = \exp[-\Phi(\vec{R}_j - \vec{R}_{j'}, \vec{\delta}, \vec{\delta}', \tau)], \quad (\text{A5})$$

$$\begin{aligned} \Phi(\vec{R}_j - \vec{R}_{j'}, \vec{\delta}, \vec{\delta}', \tau) &= \sum_{\vec{q}} |u_{\vec{q}}|^2 (1 + 2N_q) \\ &\quad - 2 \sum_{\vec{q}} v_{\vec{q}}(j, \vec{\delta}) v_{\vec{q}}^*(j', \vec{\delta}') [N_q(N_q + 1)]^{1/2} \cos[\omega_q(\tau + i\frac{\beta}{2})], \end{aligned} \quad (\text{A6})$$

where $u_{\vec{q}} \equiv (M_q/\omega_q)(e^{i\vec{q}\cdot\vec{\delta}} - 1)$ and $v_{\vec{q}}(j, \vec{\delta}) \equiv (M_q/\omega_q)e^{i\vec{q}\cdot\vec{R}_j}(e^{i\vec{q}\cdot\vec{\delta}} - 1)$.

The electron four-site correlation function $\langle c_j^\dagger(\tau)c_{j+\delta}(\tau)c_{j'+\delta'}^\dagger c_{j'} \rangle$ is easily evaluated from the Hamiltonian $\bar{\mathcal{H}}$ which transformed into the \vec{k} -space,

$$\langle c_j^\dagger(\tau)c_{j+\delta}(\tau)c_{j'+\delta'}^\dagger c_{j'} \rangle = \sum_{\vec{k}_1, \vec{k}_2} n_{\vec{k}_1} (1 - n_{\vec{k}_2}) e^{i(\vec{t}_{\vec{k}_1} - \vec{t}_{\vec{k}_2})\tau} e^{-i(\vec{k}_1 - \vec{k}_2) \cdot (\vec{R}_j - \vec{R}_{j'})} e^{i\vec{k}_2 \cdot (\vec{\delta} - \vec{\delta}')}, \quad (\text{A7})$$

where the renormalized polaron band $\vec{t}_{\vec{k}}$ is given as $t\gamma(T)\langle X_{j+\delta}^\dagger X_j \rangle \sum_{\delta} e^{i\vec{k}\cdot\vec{\delta}}$.

The time integral of the correlation functions, Eq.(7) can be performed by the saddle point approximation. In the vicinity of the saddle point, the integrand becomes just a Gaussian,

$$\Phi(\vec{R}_j - \vec{R}_{j'}, \vec{\delta}, \vec{\delta}', \tau) \simeq \xi(T) - \eta(j, j', \vec{\delta}, \vec{\delta}'; T) + \zeta(j, j', \vec{\delta}, \vec{\delta}'; T)z^2, \quad z = \tau + i\beta/2, \quad (\text{A8})$$

where $\xi(T)$, $\eta(j, j', \vec{\delta}, \vec{\delta}'; T)$, and $\zeta(j, j', \vec{\delta}, \vec{\delta}'; T)$ are, respectively, given by

$$\xi(T) = \sum_{\vec{q}} |u_{\vec{q}}|^2 (1 + 2N_q), \quad (\text{A9})$$

$$\eta(j, j', \vec{\delta}, \vec{\delta}'; T) = 2 \sum_{\vec{q}} v_{\vec{q}}(j, \vec{\delta}) v_{\vec{q}}^*(j', \vec{\delta}') [N_q(N_q + 1)]^{1/2}, \quad (\text{A10})$$

$$\zeta(j, j', \vec{\delta}, \vec{\delta}'; T) = \sum_{\vec{q}} \omega_q^2 v_{\vec{q}}(j, \vec{\delta}) v_{\vec{q}}^*(j', \vec{\delta}') [N_q(N_q + 1)]^{1/2}. \quad (\text{A11})$$

From Eqs.(7), (A5), and (A7), the dc conductivity σ is evaluated and obtained as

$$\sigma = \frac{\beta}{2} t^2 \gamma(T)^2 e^2 \sum_{\delta\delta'} \sum_{jj'} (\hat{\delta} \cdot \hat{\delta}') \sum_{\vec{k}_1 \vec{k}_2} n_{\vec{k}_1} (1 - n_{\vec{k}_2}) e^{-i\vec{k}_1 \cdot (\vec{R}_j - \vec{R}_{j'})} e^{i\vec{k}_2 \cdot (\vec{R}_j - \vec{R}_{j'} + \vec{\delta} - \vec{\delta}')} \times e^{(\tilde{t}_{\vec{k}_1} - \tilde{t}_{\vec{k}_2})/2T} e^{-(\tilde{t}_{\vec{k}_1} - \tilde{t}_{\vec{k}_2})^2/4\zeta(j,j',\vec{\delta},\vec{\delta}';T)} e^{-\xi(T)} e^{\eta(j,j',\vec{\delta},\vec{\delta}';T)} [\pi/\zeta(j,j',\vec{\delta},\vec{\delta}';T)]^{1/2}. \quad (\text{A12})$$

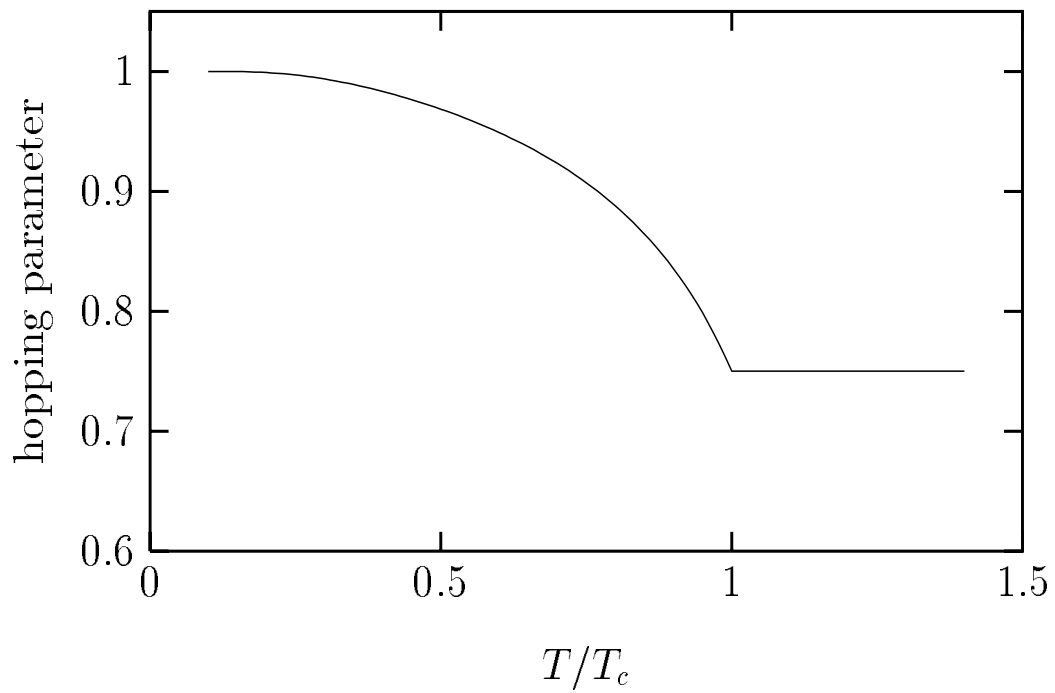
-
- [1] S. Jin, T.H. Tiefel, M. McCormack, R.A. Fastnacht, R. Ramesh, and L.H. Chen, *Science* **264**, 413 (1994).
[2] K. Chahara, T. Ohno, M. Kasai, and Y. Kozono, *Appl. Phys. Lett.* **63**, 1990 (1993).
[3] R. von Helmolt, J. Wecker, B. Holzapfel, L. Schultz, and K. Samwer, *Phys. Rev. Lett.* **71**, 2331 (1993).
[4] C. Zener, *Phys. Rev.* **82**, 403 (1951).
[5] P.W. Anderson and H. Hasegawa, *Phys. Rev.* **100**, 675 (1955); P.G. deGennes, *Phys. Rev.* **118**, 141 (1960).
[6] K. Kubo and N. Ohata, *J. Phys. Soc. Jpn.* **33**, 21 (1972).
[7] R.M. Kusters, J. Singleton, D.A. Keen, R. McGreevy, and W. Hayes, *Physica (Amsterdam)* **155B**, 362 (1989).
[8] N. Furukawa, *J. Phys. Soc. Jpn.* **63**, 3214 (1994).
[9] A.J. Millis, P.B. Littlewood, and B.I. Shraiman, *Phys. Rev. Lett.* **74**, 5144 (1995).
[10] A.J. Millis, R. Mueller, and B.I. Shraiman, *Phys. Rev. Lett.* **77**, 175 (1996); *Phys. Rev. B* **54**, 5380 (1996); *Phys. Rev. B* **54**, 5405 (1996).
[11] H. Röder, Jun Zang, and A.R. Bishop, *Phys. Rev. Lett.* **76**, 1356 (1996).
[12] J. B. Goodenough, *Metallic Oxides*, Progress in solid state chemistry, Vol.5, edited by H. Reiss (Pergamon press, Oxford 1972).
[13] H.Y. Hwang, S.-W. Cheong, P.G. Radaelli, M. Marezio, and B. Batlogg, *Phys. Rev. Lett.* **75**, 914 (1995).
[14] M.R. Ibarra, P.A. Algarabel, C. Marquina, J. Blasco, and J. Garcia, *Phys. Rev. Lett.* **75**, 3541 (1995).
[15] K.H. Kim, J.Y. Gu, H.S. Choi, G.W. Park, and T.W. Noh, *Phys. Rev. Lett.* **77**, 1877 (1996).
[16] Y.H. Jeong *et al.* (POSTECH preprint).
[17] A.P. Ramirez, P. Schiffer, S.-W. Cheong, C.H. Chen, W. Bao, T.T.M. Palstra, P.L. Gammel, D.J. Bishop, and B. Zegarski, *Phys. Rev. Lett.* **76**, 3188 (1996).
[18] G.D. Mahan, *Many-Particle Physics* (Plenum, New York, 1990).
[19] This approximation corresponds to neglecting the residual interaction between the polaron and the phonon which includes the multiphonon vertices. This approximation works well for very narrow band systems with the strong electron-phonon interaction. See A.S. Alexandrov, *Physica C* **191**, 115 (1992).
[20] W.E. Pickett and D.J. Singh, *Phys. Rev. B* **53**, 1146 (1996).
[21] S.J. Youn and B.I. Min, unpublished.
[22] D.J. Kim, *Phys. Rep.* **171**, 129 (1988).

FIG. 1. Bandwidths (hopping parameters in unit of t) as a function of the temperature. (a) Effect of the double exchange interaction, $t\gamma(T)$, ($\gamma(T) \equiv \langle \cos \frac{\theta}{2} \rangle$). (b) Combined effect of the double exchange and the electron-phonon interaction, $t\gamma(T)\Gamma(T)$. $\sum_{\vec{q}} |u_{\vec{q}}|^2 = 4.5$ is taken.

FIG. 2. The resistivity of the polaron only model (two dashed lines) and the combined model of the polaron and double exchange (solid line). In the polaron only model, \tilde{t}_{up} and \tilde{t}_{low} are the bandwidths corresponding to the the upper and lower limiting value of $\langle \cos \frac{\theta}{2} \rangle$, respectively. Calculations are performed for the parameters, $x = 0.3$, $w = 64T_c \sim 1.1\text{eV}$, $\omega_0 = 5T_c \sim 0.08\text{eV}$ assuming $T_c \sim 200\text{K}$, and $\sum_{\vec{q}} |u_{\vec{q}}|^2 = 6$. The inset presents the resistance behaviors with $H = 0\text{T}$, 4.8T , and 9.6T .

FIG. 3. (a) The phonon frequency shifts $(\tilde{\omega}_q(T) - \tilde{\omega}_q^c)/\tilde{\omega}_q^c$ for various magnetic field strengths, where $\tilde{\omega}_q^c \equiv \tilde{\omega}_q(1.1T_c, H = 0\text{T})$. In the inset, the shifts are compared with the experiment (under $H = 1\text{T}$) for $\text{La}_{0.7}\text{Ca}_{0.3}\text{MnO}_3$ (Jeong *et al.*[16]). In the fitting, $T_c = 238\text{K}$ is taken from experiments. We have taken $\bar{\beta} = 0.07$. (b) The phonon damping constants $\alpha_q(T)/\alpha_q^c$ with $\alpha_q^c \equiv \alpha_q(1.1T_c, H = 0\text{T})$, are given.

(a)



(b)

